

THE POTENTIAL OF SILICON-BASED LIGANDS IN METAL-ORGANIC FRAMEWORKS

Robert P. Davies,* Askhat Jumabekov,* Robert J. Less,* Paul D. Lickiss,* Karen Robertson,*
Karl G. Sandeman** and Andrew J. P. White*

*Chemistry Department, Imperial College, London SW7 2AZ, UK, p.lickiss@imperial.ac.uk

**Physics Department, Imperial College, London SW7 2AZ, UK, k.sandeman@imperial.ac.uk

ABSTRACT

This paper presents a description of the synthetic procedures to two silicon-based ligands and to two new metal-organic frameworks (MOFs) derived from these ligands, as well as the results of magnetic measurements on the MOFs. It was found that the new Mn(II) and Co(II) MOFs behave as paramagnets at low temperatures, and one of the compounds (**3**) experiences first order transition due to a (possible) spin crossover phenomenon.

Keywords: silicon-based ligands, metal-organic frameworks, magnetism.

1 INTRODUCTION

There is an increasing interest in the chemistry of metal-containing coordination polymers due to recent discoveries in the synthesis of new nanostructured materials known as metal-organic frameworks (MOFs). Owing to their intriguing properties such as a high porosity, high adsorption rates of different gases, and unusual magnetic properties, potential applications of these materials in fields such as gas storage, catalysis, nonlinear optics, electronics, ion exchange, and enantioselective separations are keenly anticipated [1-7].

Many MOFs are constructed from simple, commercially available, bent or linear dicarboxylic acids, which act as connecting units between metal-based nodes or metal clusters – often defined as secondary building units or SBUs – to give a three-dimensional porous network structure. The desire to better control the physical and chemical properties of the resultant networks has motivated recent research into the systematic design of new connecting ligands with specifically tailored dimensionality or pendant functional groups [8].

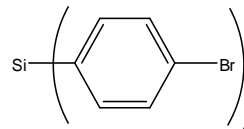
We continue to be interested in the preparation of novel silicon-based connecting units and their use in the construction of metal-containing coordination polymers. In this paper we report the synthesis of silicon-based ligands: tetrakis-4-carboxyphenylsilane (**1b**) [8] and 1,2-bis(tris-4-carboxyphenylsilyl)ethane (**2b**); and two corresponding new MOFs: **3** [8] and **4** derived from these ligands respectively.

2 EXPERIMENTAL SECTION

All reactions involving *n*-BuLi were carried out in oven-dried glassware and were performed under an atmosphere of dry nitrogen. Diethyl ether and THF were dried by distillation over sodium metal prior to use. All other reagents were commercial products that were used without further purification. NMR spectra of the ligands were recorded on a Bruker AV-400 spectrometer and mass spectra on a Micromass AutoSpec Premier. The structures of the MOFs were determined by single crystal X-ray diffraction using an Oxford Diffraction PX Ultra instrument. Magnetization measurements were carried out in an Oxford instruments VSM capable of reaching fields of ± 4 T and temperatures ranging from 4.2 to 295 K

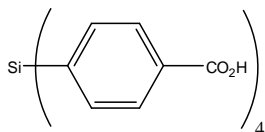
2.1 Synthesis

Synthesis of compound 1b, Si(C₆H₄CO₂H)₄ [8] A solution of *n*-butyllithium (*n*-BuLi) (42.5 ml, 2.5 M, 105 mmol, in hexane) in 50ml diethyl ether (Et₂O) was added dropwise to a solution of 1,4-dibromobenzene (25.0 g, 105 mmol) dissolved in 50 ml Et₂O at -78°C. The reaction mixture was then stirred for 1h and then warmed to 0°C. Tetraethoxysilane (5.1 ml, 21.25 mmol) was then added dropwise and the reaction mixture stirred overnight allowing the reaction mixture to warm gradually up to room temperature. The reaction was then quenched by the addition of HCl (50 ml, 1 M, 50 mmol). The organic layer was separated, washed with brine and then dried over MgSO₄. The solvent was then removed under vacuum and the resultant crude product recrystallised from EtOAc to yield a white crystalline product - tetrakis-(4-bromophenyl)silane **1a** (yield = 47%), with properties as described previously [8].



A solution of **1a** (3.7 g, 5.7 mmol) dissolved in 50 ml THF was added dropwise to a solution of *n*-BuLi (9.12 ml, 2.5 M, 22.8 mmol, in hexane) in 50 ml THF at -78°C and the reaction mixture was stirred for 1h. CO₂ was then

bubbled through the solution for a period of 2h with continued stirring and then left overnight to warm to room temperature. The reaction was quenched by the addition of HCl (50ml, 1M, 50mmol). The organic layer was separated, washed with brine, dried over MgSO₄ and all solvent removed on the rotary evaporator. The crude product **1b** was then purified by recrystallization from hot EtOAc to give a white solid with properties as described previously (yield = 70%) [8].



Synthesis of compound **2b**, [CH₂Si(C₆H₄CO₂H)₃]₂.

This compound was prepared using the same method as above starting with 25 g (106 mmol) dibromobenzene in 50 ml Et₂O, 42.5 ml (2.5 M, 106 mmol) *n*-BuLi in 50 ml Et₂O and 6.5 ml (17.5 mmol) 1,2-bis(triethoxysilyl)ethane. This gave [CH₂Si(C₆H₄Br)₃]₂ **2a** as a white powder, which was recrystallised from hot CH₂Cl₂ (yield = 59%).



Using the same method as for the previous tetra-acid, **1b**, 1.00 g (1 mmol) 1,2-bis(tris-4-bromophenylsilyl)ethane in 20 ml THF and 2.4 ml (2.5 M, 6 mmol) *n*-BuLi in 20 ml THF was used to prepare the hexa-acid. The crude product was recrystallised from EtOAc and hexane (yield = 68%)



Synthesis of MOF 3, Mn₂Si(C₆H₄CO₂)₄·H₂O. For the synthesis of the complex **3**, manganese nitrate was used as the metal salt and a mixed solvent system containing equal volumes of water and dimethylacetamide (DMA) was used. The detailed procedure is as follows: 50 mg Mn(NO₃)₂·xH₂O, 50 mg of **1b** and 4 ml 1:1 DMA:H₂O were mixed in an autoclaveable glass vessel and heated to 100°C for 18 h. The resultant large colourless needle crystals were isolated by filtration and resubmerged in fresh 1:1 DMA:H₂O solution for storage (yield = 64%).

Synthesis of MOF 4, [Co₃(OH)₂{CH₂Si(C₆H₄CO₂)₃H}₂·(H₂O)₄].9.5DMA. For the synthesis of the complex **4**, cobalt nitrate was used as the metal salt, again in a mixed solvent system comprising equal volumes of water and DMA. The detailed procedure is as follows: 5mg Co(NO₃)₂·6H₂O, 5mg of **2b** and 2ml 1:1 DMA:H₂O

were mixed in an autoclaveable glass vessel and heated to 100°C for 18 h. The resultant large purple platelet crystals were then isolated by filtration and resubmerged in fresh 1:1 DMA:H₂O solution for storage (yield = 60%).

2.2 Structure Analysis

The MOF **3** is a chain structure based on the alternation of two crystallographically distinct Mn atoms connected by O atoms of the carboxylate groups via η²(O18) and μ²(O8+O9) bonding (see Figure 1). These chains are joined together by the tetracarboxylate ligands to give a 3D network as shown in Figure 2.

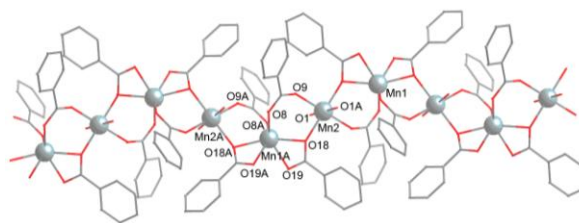


Figure 1: Ball-and-stick representation of the MnO chain of MOF **3**. Mn – blue/grey spheres, O – red stick bonds, C – grey stick bonds.

The structure of **3** is isorecticular to a structure published by Lambert *et al.* in 2008 [9,10] using the same ligand but with Zn(II) metal centres. PLATON [11] calculations show that the dehydrated sample of MOF **3** has a solvent accessible void volume of 46.1%, and is therefore slightly more porous than Lambert's Si₄Zn complex, 42.8%. The largest pores in this structure can be seen in the 001 plane measuring ca. 5 x 5 Å.

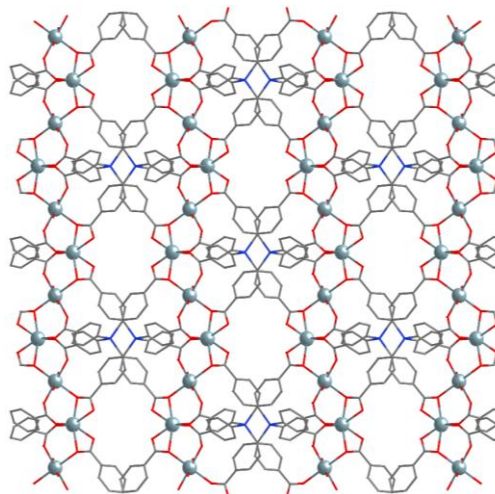


Figure 2: Ball-and-stick representation of the crystal structure of MOF **3** in the 100 plane. Mn – blue/grey spheres, Si – blue stick bonds, O – red stick bonds, C – grey stick bonds.

In contrast, the 3D structure of MOF **4** is based on trimetallic Co(II) nodes and a hexa-coordinating bis-silyl ligand. The trimetallic Co node is shown in Figure 3 and consists of 3 Co(II) centers joined by two OH anions (O73) and coordinated to 6 carboxylic acids and four terminal water molecules. There is also some disorder in this node although it does not affect the overall connectivity.

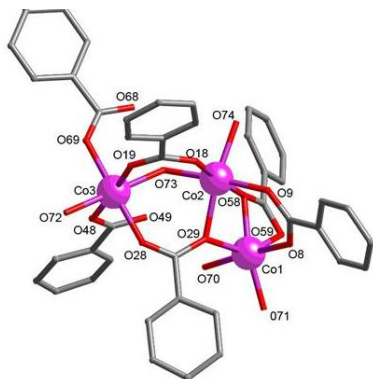


Figure 3: Ball-and-stick representation of the disordered trinuclear node of MOF **4** showing: Co – purple spheres, O – red stick bonds, C – grey stick bonds, H atoms have been omitted for clarity.

These nodes link together to form a 3D network. In the 100 plane, three channel types are present (see Figure 4) – the largest measures ca. $6 \times 8 \text{ \AA}$ and the smallest is ca. $6 \times 4 \text{ \AA}$, – the 101 direction has two channels sizes of $5 \times 5 \text{ \AA}$ and $3.5 \times 4 \text{ \AA}$ (see Figure 5). Other planes display smaller but still potentially accessible channels suggesting that this MOF has a very open structure with good possibilities for gas storage. The PLATON calculated solvent accessible void space is 56%.

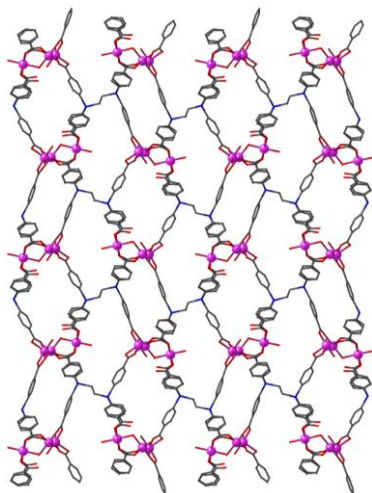


Figure 4: Ball-and-stick representation of the crystal structure of MOF **4** in the 100 plane. Co – purple spheres, O – red stick bonds, Si – blue stick bonds, C – grey stick bonds, H atoms have been omitted for clarity.

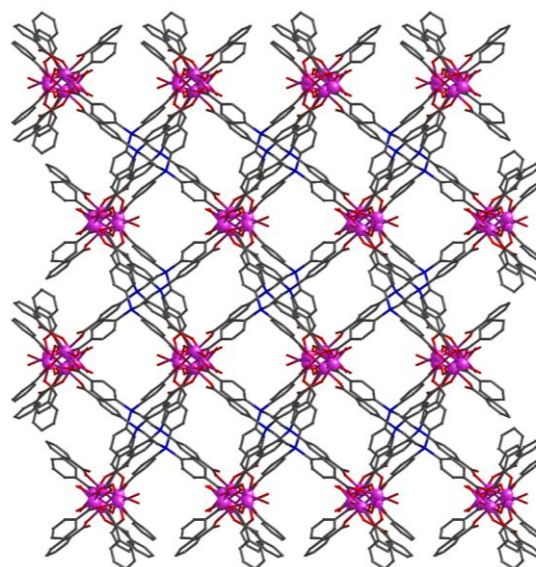


Figure 5: Ball-and-stick representation of the crystal structure of MOF **4** in the 010 plane. Co – purple spheres, O – red stick bonds, Si – blue stick bonds, C – grey stick bonds, H atoms have been omitted for clarity.

2.3 Magnetic Measurements

Measurements of magnetization (M) as a function of magnetic field strength (H) for the MOFs **3** and **4** have been performed in fields of up to $\pm 4 \text{ T}$ and temperatures ranging from 4.2 to 20 K. The isothermal dependence of magnetization on applied field $M(H)$ is shown in Figure 6 for the compound **3** and in Figure 7 for the compound **4**.

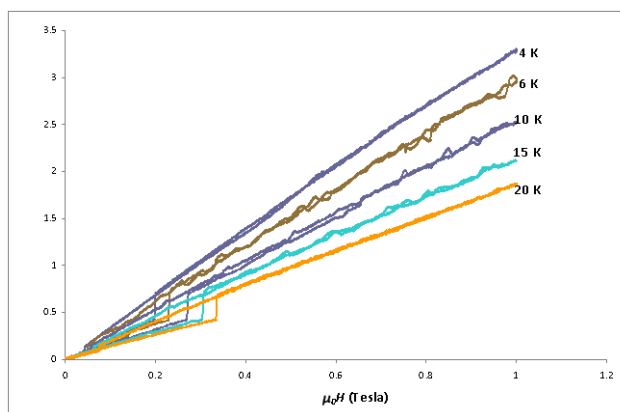


Figure 6: The magnetization of compound **3** as a function of applied magnetic field.

According to the data, compound **3** behaves as a paramagnet with a first order transition from one paramagnet state to another paramagnet state at a value of magnetization of around $0.5 \text{ Am}^2\text{kg}^{-1}$. This behavior of the compound at low temperatures might be due to a spin crossover phenomenon [12]. The estimated ratio of the

post-transition (higher field) susceptibility to the one that before transition ($\gamma = \chi_a/\chi_b$) gives a value of more than 1 for this compound. This implies that the magnitude of the spin size after the transition in **3** is larger than in low fields. Also, we estimated the entropy change ΔS due to the transition, using the magnetic Clausius-Clapeyron equation ($\Delta S = -\Delta M \times dH_c/dT$). According to this estimate, the field-induced entropy change, ΔS was negative.

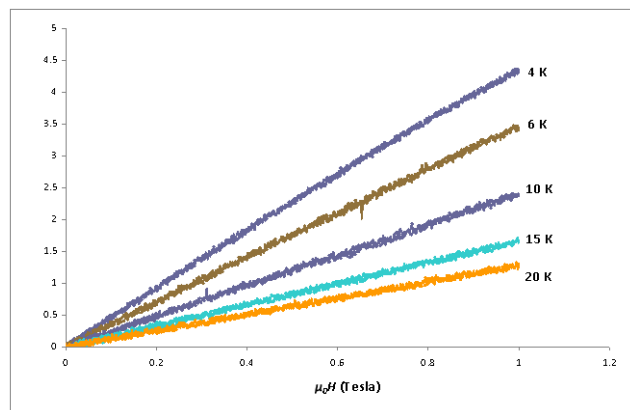


Figure 7: The magnetization of compound **4** as a function of applied magnetic field.

In the case of compound **4**, the magnetization data show that it is also a paramagnet. However, unlike the previous compound, it does not experience any transition in the range of the applied field and temperature.

3 CONCLUSIONS

The conclusions that can be drawn from this work are as follows: (i) two different silicon-based ligands have been prepared; (ii) two new MOFs have been prepared using the silicon-based ligands; (iii) the magnetic properties of the MOFs have been investigated and it was found that the compounds are a class of paramagnetic materials. However, it was observed that the compound **3** experiences a field-driven first order transition from one paramagnetic state to another at low temperatures and finite fields.

REFERENCES

- [1] S. R. Batten, S. M. Neville and D. R. Turner, *Coordination Polymers Design, Analysis and Application*, The Royal Society of Chemistry, Cambridge CB4 0WF, UK, 2009.
- [2] S. Natarajan and P. Mahata, *Chem. Soc. Rev.*, **38**, 2304-2318, 2009,
- [3] L. J. Stuart, *Chem. Soc. Rev.*, **32**, 276-288, 2003.
- [4] M. Morris, C. J. Doonan, H. Furukawa, R. Banerjee and O. M. Yaghi, *J. Am. Chem. Soc.*, **130**, 12626-12627, 2008.

- [5] J. L. C. Rowsell, J. Eckert and O. M. Yaghi, *J. Am. Chem. Soc.*, **127**, 14904-14910, 2005.
- [6] H. Li, M. Eddaoudi, M. O'Keeffe and O. M. Yaghi, *Nature*, **402**, 276-279, 1999.
- [7] M. Eddaoudi, J. Kim, N. Rosi, D. Vodak, J. Wachter, M. O'Keeffe and O.M. Yaghi, *Science*, **295**, 469-472, 2002.
- [8] R. P. Davies, R. J. Less, P. D. Lickiss, K. Robertson, and A. J. P. White, *Inorg. Chem.*, **47**, 9958-9964, 2008.
- [9] J. B. Lambert, Z. Q. Liu, and C. Q. Liu, *Organometallics*, **27**, 1464-1469, 2008.
- [10] J. B. Lambert, Y. Zhao, and C. L. Stern, *J. Phys. Org. Chem.*, **10**, 229-232, 1997.
- [11] (a) A. L. Spek, PLATON, A Multipurpose Crystallographic Tool; Utrecht University: Utrecht, The Netherlands, 2008. (b) See also: A. L. Spek, *J. Appl. Crystallogr.*, **36**, 7-13, 2003.
- [12] P. D. Southon, L. Liu, E. A. Fellows, D. J. Price, G. J. Halder, K. W. Chapman, B. Moubaraki, J.-F. Létard, and C. J. Kepert, *J. Am. Chem. Soc.*, **131**, 10998-11009, 2009.